

Article

Optical Effects Accompanying the Dynamical Bragg Diffraction in Linear 1D Photonic Crystals Based on Porous Silicon

Anton Maydykovskiy, Vladimir Novikov, Sergey Svyakhovskiy and Tatiana Murzina *

Physics Department, Moscow State University, 119991 Moscow, Russia;

E-Mails: anton@shg.ru (A.M.); novikovvb@shg.ru (V.N.); sse@shg.ru (S.S.)

* Author to whom correspondence should be addressed; E-Mail: murzina@mail.ru;
Tel.: +7-495-939-3669; Fax: +7-495-939-3113.

External Editor: Yuri Kivshar

Received: 4 August 2014; in revised form: 26 September 2014 / Accepted: 26 September 2014 /
Published: 14 October 2014

Abstract: We survey our recent results on the observation and studies of the effects accompanying the dynamical Bragg diffraction in one-dimensional photonic crystals (PhC). Contrary to the kinematic Bragg diffraction, the dynamical one considers a continuous interaction between the waves travelling within a spatially-periodic structure and is the most pronounced in the so called Laue geometry, leading to a number of exciting phenomena. In the described experiments, we study the PhC based on porous silicon or porous quartz, made by the electrochemical etching of crystalline silicon with the consequent thermal annealing. Importantly, these PhC are approximately hundreds of microns thick and contain a few hundreds of periods, so that the experiments in the Laue diffraction scheme are available. We discuss the effect of the temporal splitting of femtosecond laser pulses and show that the effect is quite sensitive to the polarization and the phase of a femtosecond laser pulse. We also show the experimental realization of the Pendular effect in porous quartz PhC and demonstrate the experimental conditions for the total spatial switching of the output radiation between the transmitted and diffracted directions. All described effects are of high interest for the control over the light propagation based on PhC structures.

Keywords: dynamical Bragg diffraction; photonic crystals; pulse splitting; Pendular effect

1. Introduction

Effects of light propagation through photonic crystals (PhC) have been intensively studied in last decades. They reveal a number of exciting phenomena that originate generally from the spatial periodicity of the PhC structure. First of all one should mention here the dispersion modulation in definite frequency-angular spectral intervals, that are close to the edges of the so called photonic band gap [1,2]. This leads to such well known effects as slow light, *i.e.*, a substantial decrease of the light group velocity [3], spatial and spectral light localization [4], the decrease of the optical excitation threshold of PhC based laser structures [5,6]. An important property of photonic crystals is also a manifold amplification of the efficiency of the nonlinear-optical effects such as harmonics' generation [7,8] and nonlinear magneto-optical effects [9]. When the nonlinear interaction of the pulsed laser radiation with the PhC structure is sufficient, the so-called gap solitons can exist within the photonic crystals [10,11]. These peculiarities of light-PC interaction are prospective for the development of new methods for the operation over propagation of the light flow.

A specific area in the context of the light-PhC interaction is the dynamical Bragg diffraction of the electromagnetic waves in a spatially periodic medium, which originates from a strong coupling between the coherent diffracted waves existing in a PhC, often named Borrmann and anti-Borrmann modes and which are localized within the layers with low and high refractive indices, respectively. It may be realized for the Laue transmission scheme, when the electromagnetic radiation propagates in the direction parallel to the PC layers under the fulfillment of the Bragg diffraction conditions. It is known from the X-ray research area that in this experimental geometry the so-called pendulum effect can exist, which is a periodic oscillation of the energy between the transmitted and diffracted waves in a PhC [12,13]. This effect is of special interest for an all-optical switching of laser pulses propagating inside a PhC. Borrmann effect is also a well-known phenomenon observed for the dynamical Bragg diffraction conditions for the X-rays [14]. Recently, a perspective optical phenomenon of diffraction-induced laser pulses splitting (DIPS) under the dynamical Bragg diffraction in the Laue scheme of diffraction in a linear one-dimensional (1D) PC was described theoretically [15,16]. It was shown that short (femtosecond) laser pulses after passing through a PhC can be split into two, the separation time being determined by the PhC properties.

In this paper we discuss our recent results on the experimental observation and studies of the pendulum and DIPS effects along with their pronounced polarization selectivity in the Laue geometry in 1D photonic crystals.

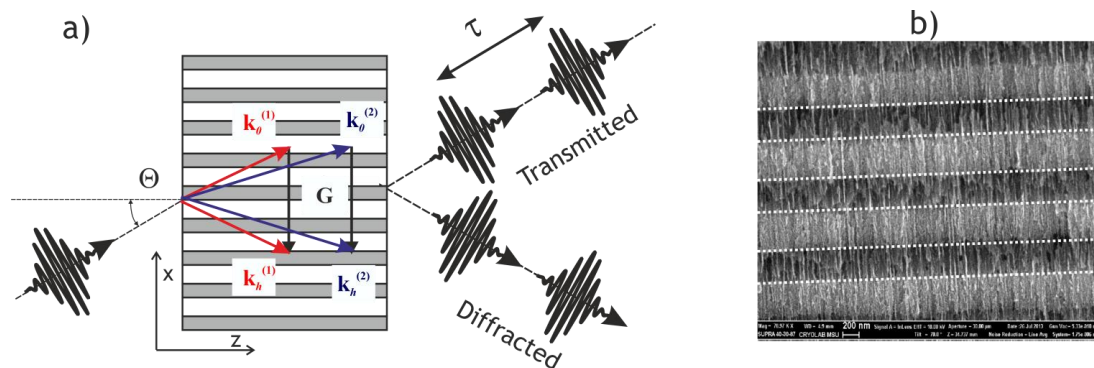
2. Dynamical Bragg Diffraction in Linear 1D PhC: The Main Approach

The optical effects discussed below for the Laue geometry of the Bragg diffraction came mostly from the X-ray spectral range. The corresponding theory was also developed, which could be to some extent applied to the optical wavelength range. Still the following quite important differences should be clarified. The most important one is that the value of the variation of the refractive index modulation for the case of photonic crystals is quite large (can be over 10%), that is approximately four orders of magnitude higher as compared to the X-rays spectral range for the electronic crystals. One of the important circumstances of this property, as was shown in [15], is a high spatial inhomogeneity of the

distribution of optical field within a PC, so that a single incident short laser pulse splits into two that propagate in a photonic crystal with different group velocities, that was named the diffraction induced pulse splitting (DIPS).

Importantly, that the fast (Borrmann) pulse is formed by the two coupled diffracted waves that are localized in PC layers with smaller refractive index, while the slow (anti-Borrmann) pulse is formed by the interacting waves that are concentrated predominantly within the layers with high refractive index. This is shown schematically in Figure 1a. In the case of a large enough pulse propagating length inside a PC, the splitting time between the Borrmann and of the anti-Borrmann pulses can be large enough and be detected in the experiment.

Figure 1. (a) Scheme of the dynamical Bragg diffraction and of the temporal pulse splitting in the direct and diffraction directions; (b) SEM image of the cross-section of the porous silicon based PhC.



Theoretical description of the dynamical Bragg diffraction was developed recently (see [15,16] and references therein). It is based on solving the boundary problem of the interacting fields for the Laue geometry and for the spatially confined laser pulses. Briefly, the incident laser pulse at the PC surface (*i.e.*, at $z = 0$) is taken in the form of a two-dimensional Fourier expansion, that is as a series of monochromatic plane waves that correspond to the frequency interval $[\omega_0 \pm \Omega]$, where ω_0 is the central frequency, $\Omega \ll \omega_0$, and with the amplitudes that are the functions of the coordinates z , x and of the time t ; the coordinate system is shown in Figure 1a as well. In the frame of the two-wave approximation and under the fulfillment of the Bragg diffraction condition, $\sin \vartheta_B = \lambda/2d$, d being the PC period, the p -polarized electric field within the bulk of the photonic crystal is determined by the expression [16]:

$$\mathbf{E}(x, z, t) = \{ \mathbf{E}_0(x, z, t) + \mathbf{E}_h(x, z, t) \exp(-i G x) \} \times \exp(i k_{0x} x - i \omega_0 t) \quad (1)$$

where $G = 2\pi/d$ is the reciprocal lattice vector, $\mathbf{E}_0(x, z, t)$ and $\mathbf{E}_h(x, z, t)$ are the amplitudes of the transmitted and diffracted waves, respectively; the wave vector $k = \omega/c = k_{0x} + K$, $k_{0x} = k_0 \sin \theta$ is the lateral projection of the wave vector, θ is the angle of incidence. In other words, a coherent superposition of the incident, E_0 , and of the diffracted, E_h , pulse fields determine the field in every point within the PhC structure. This two-wave approximation is valid in particular due to an achievable large modulation of the permittivity (of the refraction index) of the layers that compose the photonic crystal. The permittivity of the PhC in this approximation is:

$$\varepsilon(x) = \varepsilon_0 + \varepsilon_h \exp(-i h x) + \varepsilon_{-h} \exp(i h x) \quad (2)$$

where ε_0 , ε_h , ε_{-h} are the spatial Fourier components of the permittivity, the exact equations that determine their dependence on the PhC material and geometrical parameters of a particular structure are described in [16]. Importantly, the amplitudes of the confined fields $\mathbf{E}_0(x, z, t)$ and $\mathbf{E}_h(x, z, t)$ are given by integrating over the frequency-angular distribution of the propagating pulses, thus giving the dependence of the output field on both the dielectric parameters of the photonic crystal, as well as on the duration, phase, amplitude and propagation direction of the incident pulsed radiation.

3. Composition of Multilayer Porous Silicon Based 1D Photonic Crystals

In this work we performed the experiments for the 1D PhC based on porous quartz. The technique of the composition of such structures is well known and is described in detail elsewhere (see, for example, [17] and references therein). It is based on the electrochemical etching of crystalline (001) *p*-type silicon of the resistivity of about 0.005 Ω cm in HF-based electrolyte (HF:H₂O:ethanol in the ratio 2:4:3 for the HF concentration of 21% (w/w)), which results in the formation of pores oriented along the [100] direction, *i.e.*, perpendicularly to the surface of the Si(001) plate. During this procedure, the silicon plate serves as the bottom electrode, while the platinum wire is the second electrode in a two-electrode electrochemical cell. It was checked that the pores' diameter and thus the porosity of the porous silicon layer are proportional to the electrochemical current density, while the etching time determines the depth of the pores. Thus, the periodic modulation of the current density results in the formation of spatially periodic porous structure, the layers of the constant porosity being oriented parallel to the Si(001) surface. The average pores' diameter in our conditions were varied in the interval 10–60 nm [18], which is much smaller than the optical wavelength, so that such porous layers may be treated as a homogeneous media. As a result, the PC made of several hundreds of layers with low porosity (high refractive index, n_1) and of high porosity (smaller refractive index, n_2) was made, its average thickness being about 300 microns.

When fabricating the PhC structures for the experiments in the Laue geometry of the Bragg diffraction, the following requirements were considered. First, the PhC should contain a large number of layers, so that the cross-section of the structure would be large enough to carry out the optical experiments, where the laser spot diameter is of dozens of microns. Second, the optical thickness of the layers was made to satisfy the relation $n_1 d_1 = n_2 d_2 = \lambda/4$, where λ is the central wavelength of the photonic band gap and determines the Bragg condition and is close to 800 nm, which is the fundamental wavelength of our laser systems. As a result, a high periodic structure is formed; the cross-section is shown in Figure 1b.

Most of the optical experiments were performed when using the output radiation of a Ti-sapphire laser at 800 nm, where the absorption of (porous) silicon is large enough. In order to make the PhC structure transparent at this wavelength, we performed a thermal annealing of the structure at $T = 900$ °C for a couple of hours. It was proven that annealing does not break the structural periodicity of the PhC, while leads to a substantial decrease of the refractive index of the porous layers and consequently to a spectral shift of the photonic band gap and Bragg diffraction condition. Thus the corresponding calibration measurements and the necessary corrections of the thicknesses of the porous silicon layers of the composed PhC were made for a required spectral range.

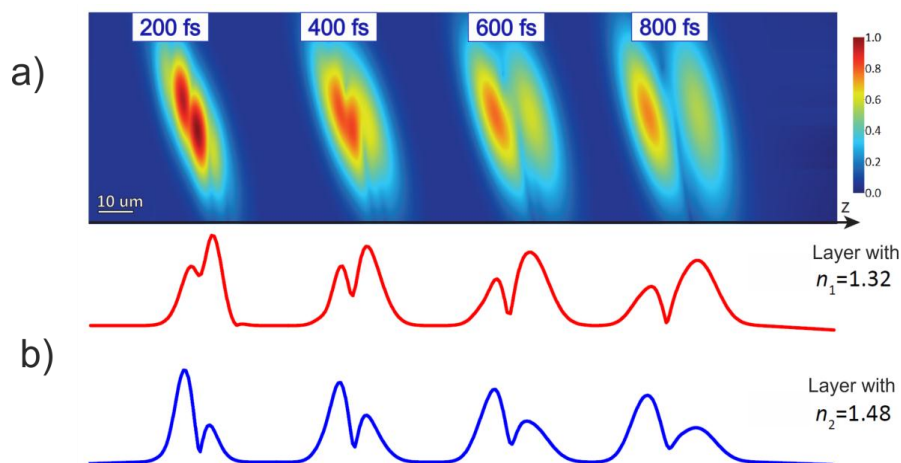
4. Experimental Results

4.1. Temporal Splitting of the Femtosecond Laser Pulses

The experiments on the temporal splitting of short laser pulses were performed for a 1D porous quartz based PhC 300 μm thick (consisting of 375 periods of 390 nm thick), the refractive indexes of the alternating layers being $n_1 = 1.45$ and $n_2 = 1.35$. The radiation of a Ti-sapphire laser at the wavelength of 800 nm and the pulse duration of 30 fs was used, which was focused on a cut-off of a PhC structure into a spot of approximately 30 μm in diameter. The diffraction Bragg condition was realized at the angle of incidence of 31° .

Prior to the experimental studies, FDTD calculations were performed in order to model the process, the parameters of the sample, of the angle of incidence of 30 fs laser pulses being the same as in the experiment. The corresponding results of the instantaneous spatial distribution of the amplitude squared of the propagating pulse are shown in Figure 2 for different time intervals after the entrance of the laser pulses into the PhC. It can be seen that for the times above approximately 400 fs the input pulse is clearly separated into two ones.

Figure 2. Finite difference time domain (FDTD) calculation of the propagation of a 30 fs laser pulse through a PhC in the Laue scheme of the dynamical Bragg diffraction; the PhC layers are parallel to the z -axis (shown in panel a) and perpendicular to the plane of the figure. (a) Spatial distribution of the pulse intensity after the laser pulse travels for 200 fs, 400 fs, 600 fs and 800 fs inside a PhC; (b) cross-sections of the panel a made for the layers of low porosity (upper red curve) and of high porosity (bottom blue curve).



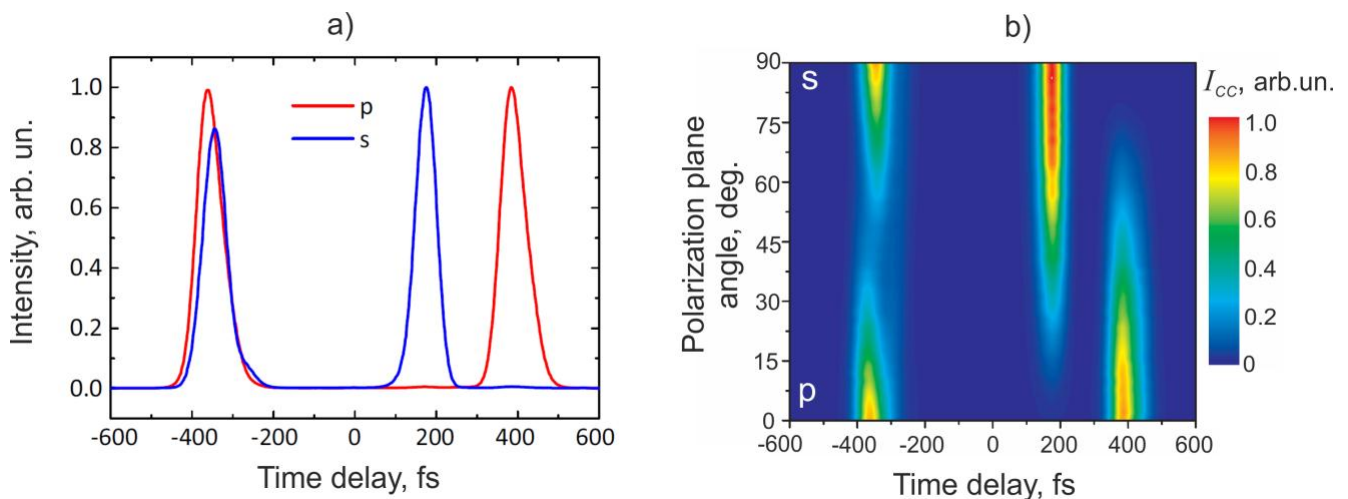
Most evidently it can be seen on the cross-sections of the 3D distribution (see Figure 2b), where we present the intensity distribution calculated for the coordinates x that correspond to the centers of layers with low and high refractive index. It stems from Figure 2b that the first (“fast”) pulse from a pair is concentrated mostly in layers with low n and corresponds to the Borrmann mode. On the contrary, the second (“slow”) pulse is localized predominantly in more optically dense layers and thus is associated with the anti-Borrmann mode.

Experiments were performed using the cross-correlation scheme based on a Ti-sapphire laser, the pulse width in the signal and reference arms being of 30 fs. The sample was placed in the signal arm in

the Laue diffraction geometry, the laser radiation was focused onto its facet into a spot of 20 μm in diameter. The cross correlation function was studied when measuring the intensity of the second harmonic generated in a BBO crystal under the noncollinear synchronism, as the pulses passed through the PhC and the reference arms were focused on it and as the time delay τ between the pulses from the signal and the reference arms was varied: $I_{CC}(\tau) \propto \int_{-\infty}^{\infty} I_S(t) I_R(t + \tau) dt$, where $I_S(t)$ and $I_R(t + \tau)$ are the pulse intensities in the signal and the reference channels.

Figure 3a shows the cross-correlation functions measured for the *s*- and *p*-polarized fundamental radiation. In both cases the diffraction-induced pulse splitting (DIPS) effect is observed, while the separation time is different for the two polarizations and is $\tau_{12}^{(p)} \approx 746$ fs for the *p*-polarized fundamental radiation and $\tau_{12}^{(s)} \approx 520$ fs for the *s*-polarization.

Figure 3. (a) Cross-correlation functions measured for the *p*- and *s*-polarized fundamental radiation and (b) as a function of the angle between the polarization plane of the fundamental radiation and the plane of incidence.



This same effect is evident from Figure 3b, which shows the dependence of the cross-correlation function on the polarization of the incident pulsed radiation and a continuous transformation of the output pulse splitting for the cases of the *p*- and *s*-polarizations. In particular, for the *mixed* polarization (polarization plane is tilted to 45° with respect to the plane of incidence) the output pulse is split temporally into three.

The mechanism underlying the observed polarization sensitivity of the DIPS effect, namely that the time splitting is approximately 1.5 times larger for the case of *p*-polarization, is two-fold, as was discussed in [19]. First, it is induced by the lattice anisotropy of a 1D PhC. It appears from the full expression for the wave equation if we consider, that $\nabla \times \nabla \times \mathbf{E}(r, t) = -\Delta \mathbf{E}(r, t) - \nabla (\epsilon^{-1} (\nabla \epsilon) \mathbf{E}(r, t))$, *i.e.*, as the gradient of the dielectric permittivity is taken into consideration. The following expressions for the time splitting in the DIPS effect were obtained [19]:

$$\tau_{12}^{(s)} = \frac{z \epsilon_h}{c \epsilon_0^{1/2}} \left(1 - \frac{\sin^2 \vartheta_B}{2 \epsilon_0} \right); \quad \tau_{12}^{(p)} = \frac{z \epsilon_h}{c \epsilon_0^{1/2}} \left(1 + 3 \frac{\sin^2 \vartheta_B}{2 \epsilon_0} \right) \quad (3)$$

where z is the PhC length and ε_0 , ε_h are the zero and the first spatial Fourier components of the permittivity, and c is the speed of light.

Second, we have to take into consideration the *material* anisotropy of porous quartz. Previous studies [20,21] as well as our experiments [22] have shown that it is quite significant in our case, so that for the refractive indices for the ordinary and extraordinary beams are $n_{1,0} = 1.35 \pm 0.01$; $n_{1,e} = 1.32 \pm 0.01$ and $n_{2,0} = 1.46 \pm 0.01$; $n_{2,e} = 1.45 \pm 0.01$. The performed calculations show a good correlation with the experimental dependencies if both types of anisotropy are considered.

4.2. Dynamical Bragg Diffraction of Chirped Femtosecond Laser Pulses: The Effect of Selective Pulse Compression

Recently it was predicted that the dynamical Bragg diffraction should lead to distinct effects for the propagation of chirped pulses in a PhC, namely, compression or decompression of the pulses after passing through a PhC may be observed depending in the chirp sign [16]. Below we show the experimental evidence of this effect, first reported in [23].

The PhC used for these experiments and the cross-correlation scheme were similar to described in the previous section. The phase modulation of the laser pulse in the signal arm was introduced by a four-prism compressor, which allowed to modulate the pulse width in the interval 35–140 fs when keeping constant the pulse spectral width; the linear phase modulation (chirp) can be characterized by the parameter $\beta = \phi'' (\Delta\omega)^2 \approx \pm \sqrt{(\tau/\tau_0)^2 - 1}$, where τ_0 , τ are the pulse duration prior to the compression and after it, correspondingly, ϕ'' is the second phase derivative, that is the group delay dispersion, $\Delta\omega$ is the pulse spectral width. The compressed signal pulse was focused on the PhC facet into a spot of 20 μm in diameter. The pulse duration in the reference channel was kept to be 30 fs.

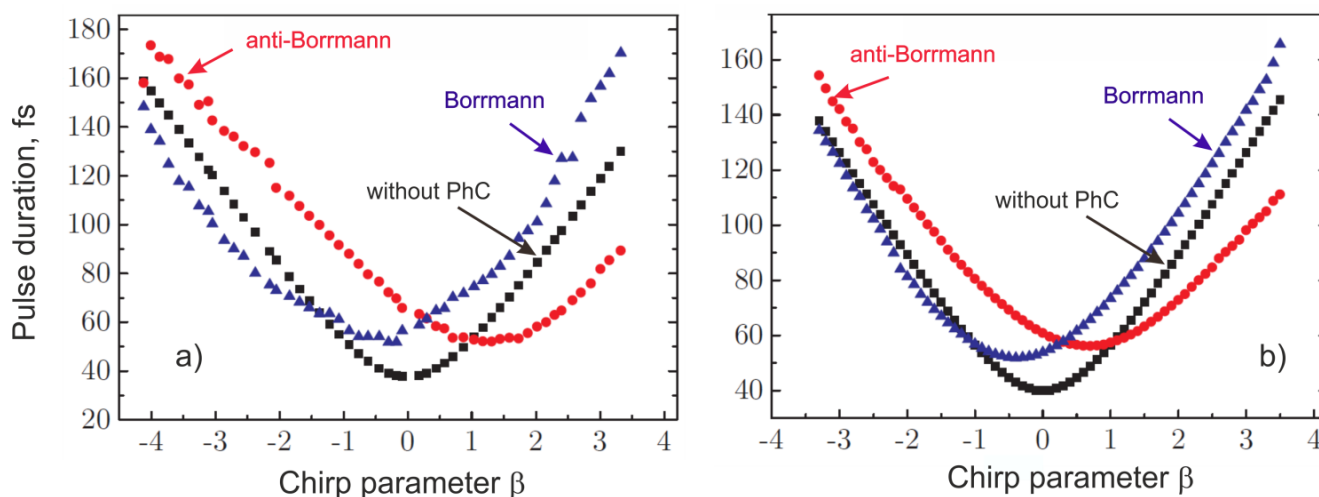
Figure 4a shows the dependencies of the widths of the Borrmann and of the anti-Borrmann pulses that are observed after passing through the photonic crystal; pulse duration were estimated from the deconvolution of the measured cross-correlation functions for various values of the chirp parameter β . For the comparison, the estimated pulse duration measured without a PhC in the signal arm is shown in the same graph. It can be seen that in general the pulse widths of the first (Borrmann) and the second (anti-Borrmann) outgoing pulses for every β value are different. Namely, for $\beta < 0$ the Borrmann pulse is compressed up to the duration of 80 fs, while the laser pulse measured without the sample in the sample channel is about 96 fs. At the same time, the duration of the anti-Borrmann pulse exceeds 120 fs under the same experimental conditions.

In other words, we observe the effect of the selective pulse compression (decompression).

For positive chirp values the situation is reversed. At zero β the duration of both the Borrmann and of the anti-Borrmann pulses are equal to each other within the experimental accuracy; it exceeds the pulse width of the reference laser pulse due to the material dispersion of the photonic crystal.

The results of the FDTD calculations of the spatial widths of the Borrmann and anti-Borrmann pulses for the experimentally realised conditions are shown in Figure 4b. They reveal a good correlation with the experimental data and also testify the observation of the effect of selective compression of chirped laser pulses in the Laue scheme of the Bragg diffraction.

Figure 4. (a) Experimental and (b) calculated dependencies of the values of the duration of the Borrmann, anti-Borrmann and input chirped pulses on the chirp parameter β .



4.3. Pendulum Effect in the Laue Diffraction Scheme in 1D Porous Silicon PhC

The pendulum (Pendellösung) effect, which is well-known from X-ray optics, consists in a periodic exchange of energy between the transmitted and diffracted waves, which are shown schematically in Figure 1a. To some extent it is analogous to the behavior of a mechanical system consisting of two coupled pendulums; in optics it is described by the dynamical Bragg diffraction theory. Recently the pendulum effect in microwaves was studied for 2D photonic crystal made of an array of aluminum cylinders [13,24], while only a few periods of the electromagnetic field beating within a PhC were observed. A possibility of making polarizing beam splitter based of the Pendellösung effect in a photonic crystal is considered theoretically and numerically in [25], where the possibility to achieve the negative refraction in a PhC is exploited. The concept of this effect is close to the so called superprism effect in PhC [26,27]. The observation of the pendulum effect in the optical range reported in [25] for a holographic grating was still related to a relatively low contrast of the refractive index in the structure so that a small number of periods of the oscillations were achieved.

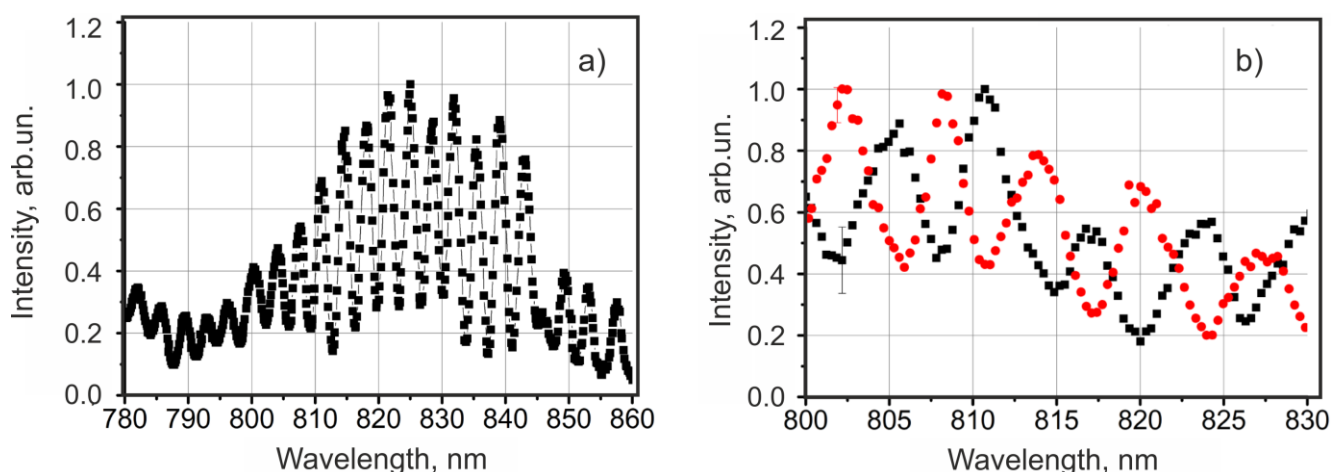
Below we describe the results on the studies of the Pendellösung effect in a 1D linear photonic crystal (PC) at the Laue diffraction scheme.

The experiments were made for a 1D linear PhC based on porous quartz and similar to described in Section 4.1, the length of the PhC sample being about 0.3 mm. An OPO laser system with a pulse duration of 10 ns and with the wavelength (idler) tuning range from 720 nm up to 1200 nm was used as the light source. In order to decrease the spectral width of the incident beam, a spatial filter was introduced in front of the sample, so that the line width of about 1 nm was used. The studies of the pendulum effect were performed close to the Bragg diffraction condition, which is at 30° angle of incidence and close to the wavelength of 800 nm. After the sample, the intensity of the transmitted and diffracted beams was detected using the photodiodes. The polarization of the incident radiation was controlled by the double Fresnel rhombus.

Figure 5a shows the spectral dependence of the intensity of the diffracted beam when *s*-polarized fundamental radiation was used. It reveals intensity oscillations with the average period of $\Delta\tau = 3.56 \pm 0.01$ nm, which is much smaller than the previously reported values. Similar spectra were

measured simultaneously for the two outgoing channels (see Figure 5b), which shows that the oscillations in the transmitted and diffracted beams are in antiphase and their periods are equal to each other. This proves that the observed phenomenon is the Pendellösung effect.

Figure 5. (a) Intensity spectrum of the diffracted beam passed through the porous quartz PhC of 0.2 mm long in the Laue geometry; (b) spectra of the transmitted (red symbols) and of diffracted (black symbols) beams under measured under the similar conditions.



It is worth noting that the intensity modulation depth of these dependencies is rather high and reaches 60%, that is quite enough for a reliable detection of the spatial switching of the laser beam between the transmitted and diffracted directions when varying the wavelength of the incident radiation. Similar dependencies were attained for the *p*-polarized fundamental beam, while the oscillation period is larger and is about 6 nm for the chosen experimental geometry [28]. This is again due to the material dispersion of the porous quartz PhC.

The period of the Pendulum effect in a PhC is determined by the expression

$$2\Lambda^{(s,p)} = 2\pi / \Delta q_z^{(s,p)} = 2\pi / (q_{z1}^{(s,p)} - q_{z2}^{(s,p)}) \quad (4)$$

where $\Lambda^{(s,p)}$ is the extinction length and $q_{z1}^{(s,p)}$, $q_{z2}^{(s,p)}$ are the *z*-projections of the wave vectors of the Borrmann and of the anti-Borrmann *p*- or *s*-polarized waves within the photonic crystal. Figure 5 demonstrates the pendulum effect induced by the variation of the wavelength of light incident on the photonic crystal, while qualitatively similar dependencies can be realized for say when changing continuously the length of the PhC structure [28].

While the physics underlying the observed Pendular effect in linear 1D PhC is known, still the results shown in Figure 5 are new and rather promising. In fact, a wide flexibility of the electrochemical technique that is used for the composition of porous quartz photonic crystals allows for the fabrication of an optical spatial splitter for the desired spectral range. Wide flexibility of the fabrication procedure is supported by the usage of the electrochemical etching technique in combination with the thermal annealing, which allows to vary easily both the optical and “physical” thickness of the PhC layers. Moreover, the period of the intensity redistribution between the transmitted and diffracted beams, which is proportional to the extinction parameter of the PhC, can be controlled by choosing the thickness of the PhC structure.

5. Conclusions

Summing up, we have studied a number of linear optical effects accompanying the dynamical Bragg diffraction of light in the Laue geometry in porous quartz based photonic crystals. Namely, the experimental observation of the temporal splitting of the femtosecond laser pulses and its polarization sensitivity, selective compression (decompression) of the temporally split pulses with the linear phase modulation, and the pendulum effect with a small spectral period of a few nanoseconds are discussed. The observed phenomena are very promising for the control over the propagation of the laser radiation, both for the short (femtosecond) pulses and for a continuous radiation as well.

Acknowledgments

This work was in part supported by RFBR, grant No. 13-02-00300.

Author Contributions

Anton Maydykovskiy, Vladimir Novikov and Sergey Svyakhovskiy have made all the experiments; Vladimir Novikov and Sergey Svyakhovskiy performed the calculations; all of them took part in the paper writing under the leadership of Tatiana Murzina.

Conflicts of Interest

The authors declare no conflict of interest.

References

1. Sakoda, K. *Optical Properties of Photonic Crystals*, 2nd ed.; Springer: Berlin, Germany, 2004.
2. Joannopoulos, J.D.; Johnson, S.G.; Winn, J.N.; Meade, R.D. *Photonic Crystals: Molding the Flow of Light*, 2nd ed.; Princeton University Press: Princeton, NJ, USA, 2008.
3. Gersen, H.; Karle, T.J.; Engelen, R.J.; Bogaerts, W.; Korterik, J.P.; van Hulst, N.F.; Krauss, T.F.; Kuipers, L. Real-space observation of ultraslow light in photonic crystal waveguides. *Phys. Rev. Lett.* **2005**, *94*, doi:10.1103/PhysRevLett.94.073903.
4. Yeh, P.; Yariv, A.; Hong, C. Electromagnetic propagation in periodic stratified media. I. General theory. *J. Opt. Soc. Am.* **1977**, *67*, 423–438.
5. Yablonovitch, E. Inhibited spontaneous emission in solid-state physics and electronics. *Phys. Rev. Lett.* **1987**, *58*, 2059–2062.
6. Zhu, L.; Chak, P.; Poon, J.K.S.; DeRose, G.A.; Yariv, A.; Scherer, A. Electrically-pumped, broad-area, single-mode photonic crystal lasers. *Opt. Express* **2007**, *15*, 5966–5975.
7. Scalora, M.; Bloemer, M.J.; Manka, A.S.; Dowling, J.P.; Bowden, C.M.; Viswanathan, R.; Haus, J.W. Pulsed second harmonic generation in nonlinear one-dimensional periodic structures. *Phys. Rev. A* **1997**, *56*, 3166–3174.
8. Soboleva, I.V.; Murchikova, E.M.; Fedyanin, A.A.; Aktsipetrov, O.A. Second- and third-harmonic generation in birefringent photonic crystals and microcavities based on anisotropic porous silicon. *Appl. Phys. Lett.* **2007**, *87*, 241110:1–241110:3.

9. Inoue, M.; Fujikawa, R.; Baryshev, A.; Khanikaev, A.; Lim, P.B.; Uchida, H.; Aktsipetrov, O.; Fedyanin, A.; Murzina, T.; Granovsky, A. Magnetophotonic crystals. *J. Phys. D Appl. Phys.* **2006**, *39*, doi:10.1088/0022-3727/39/8/R01.
10. Kivshar, Y.S.; Agrawal, G.P. *Optical Solitons: From Fibers to Photonic Crystals*; Academic: Waltham, MA, USA, 2003.
11. Mok, J.T.; de Sterke, C.M.; Eggleton, B.J. Delay-tunable gap-soliton-based slow-light system. *Opt. Express* **2006**, *14*, 11987–11996.
12. Calvo, M.L.; Cheben, P.; Martínez-Matos, O.; Monte, F.; Rodrigo, J.A. Experimental Detection of the Optical Pendellosung Effect. *Phys. Rev. Lett.* **2006**, *97*, doi:10.1103/PhysRevLett.97.084801.
13. Savo, S.; di Gennaro, E.; Miletto, C.; Andreone, A.; Dardano, P.; Moretti, L.; Mocella, V. Pendellosung effect in photonic crystals. *Opt. Express* **2008**, *16*, 9097–9105.
14. Borrmann, G. Über Extinktionsdiagramme der Röntgenstrahlen von Quarz. *Phys. Z.* **1941**, *42*, 157–162. (In German)
15. Bushuev, V.A.; Mantsyzov, B.I.; Skorynin, A.A. Diffraction-induced laser pulse splitting in a linear photonic crystal. *Phys. Rev. A* **2009**, *79*, doi:10.1103/PhysRevA.79.053811.
16. Skorynin, A.A.; Bushuev, V.A.; Mantsyzov, B.I. Dynamical Bragg diffraction of optical pulses in photonic crystals in the Laue geometry: Diffraction-induced splitting, selective compression, and focusing of pulses. *J. Exp. Theor. Phys.* **2012**, *115*, 56–67.
17. Pavesi, L. Porous silicon dielectric multilayers and microcavities. *Riv. Nuovo Cimento* **1997**, *20*, 1–76.
18. Svyakhovskiy, S.E.; Maydykovskiy, A.I.; Murzina, T.V. Mesoporous silicon photonic structures of thousands of periods. *J. Appl. Phys.* **2012**, *112*, doi:10.1063/1.4732087.
19. Svyakhovskiy, S.E.; Kompanets, V.O.; Maydykovskiy, A.I.; Murzina, T.V.; Chekalin, S.V.; Skorynin, A.A.; Bushuev, V.A.; Mantsyzov, B.I. Observation of the temporal Bragg-diffraction-induced laser-pulse splitting in a linear photonic crystal. *Phys. Rev. A* **2012**, *86*, doi:10.1103/PhysRevA.86.013843.
20. Timoshenko, V.Y.; Osminkina, L.A.; Efimova, A.I.; Golovan, L.A.; Kashkarov, P.K.; Kovalev, D.; Kunzner, N.; Gross, E.; Diener, J.; Koch, F. Anisotropy of optical absorption in birefringent porous silicon. *Phys. Rev. B* **2003**, *67*, doi:10.1103/PhysRevB.67.113405.
21. Golovan, L.A.; Melnikov, V.A.; Konorov, S.O.; Fedotov, A.B.; Timoshenko, V.Y.; Zheltikov, A.M.; Kashkarov, P.K.; Ivanov, D.A.; Petrov, G.I.; Yakovlev, V.V. Linear and nonlinear optical anisotropy of amorphous oxidized silicon films induced by a network of pores. *Phys. Rev. B* **2006**, *73*, doi:10.1103/PhysRevB.73.115337.
22. Svyakhovskiy, S.E.; Skorynin, A.A.; Bushuev, V.A.; Chekalin, S.V.; Kompanets, V.O.; Maydykovskiy, A.I.; Murzina, T.V.; Novikov, V.B.; Mantsyzov, B.I. Polarization effects in diffraction-induced laser pulse splitting in one-dimensional photonic crystals. *JOSA B* **2013**, *30*, doi:10.1364/JOSAB.30.001261.
23. Svyakhovskiy, S.E.; Maydykovskiy, A.I.; Novikov, V.B.; Kompanets, V.O.; Chekalin, S.V.; Skorynin, A.A.; Bushuev, V.A.; Mantsyzov, B.I.; Murzina, T.V. Selective Compression of Femtosecond Laser Pulses in a Linear Photonic Crystal. In Proceedings of the Frontiers in Optics FTu3A.21, Orlando, FL, USA, 6–10 October 2013.

24. Mocella, V. Negative refraction in Photonic Crystals: Thickness dependence and Pendellosung phenomenon. *Opt. Express* **2005**, *13*, 1361–1367.
25. Mocella, V.; Dardano, P.; Moretti, L.; Rendina, I. A polarizing beam splitter using negative refraction of photonic crystals. *Opt. Express* **2005**, *13*, 7699–7707.
26. Merzlikin, A.M.; Vinogradov, A.P. Superprism effect in 1D photonic crystal. *Opt. Commun.* **2006**, *259*, 700–703.
27. Panoiu, N.C.; Bahl, M.; Osgood, R.M. Optically tunable superprism effect in nonlinear photonic crystal. *Opt. Lett.* **2003**, *28*, 2503–2505.
28. Novikov, V.B.; Svyakhovskiy, S.E.; Skorynin, A.A.; Bushuev, V.A.; Mantsyzov, B.I.; Maydykovskiy, A.I.; Murzina, T.V. Control over the Light Propagation by Means of the Pendellosung Effect in 1D Porous Quartz Photonic Crystal. In Proceedings of the ICONO/LAT 2013, Moscow, Russia, 18–22 June 2013.

© 2014 by the authors; licensee MDPI, Basel, Switzerland. This article is an open access article distributed under the terms and conditions of the Creative Commons Attribution license (<http://creativecommons.org/licenses/by/4.0/>).